Extracellular Calcium Depletion as a Mechanism of Short-Term Synaptic Depression

RICHARD D. KING,* MICHAEL C. WIEST,* AND P. READ MONTAGUE
Center for Theoretical Neuroscience, Division of Neuroscience, Baylor College of Medicine, Houston, Texas 77030

Received 25 September 2000; accepted in final form 4 January 2001

King, Richard D., Michael C. Wiest, and P. Read Montague. Extracellular calcium depletion as a mechanism of short-term synaptic depression. *J Neurophysiol* 85: 1952–1959, 2001. Recent experiments have demonstrated that normal neural activity can cause significant decrements in external calcium levels, and that these decrements mediate a form of short-term synaptic depression. These findings raise the possibility that certain forms of short-term synaptic depression at glutamatergic synapses throughout the mammalian CNS may be influenced by similar changes in external calcium. We use a computational model of the extracellular space, combined with experimental data on calcium consumption, to show that such short-term depression can be accounted for by changes in calcium just outside active synapses, provided that external calcium diffusion is restricted. Remarkably, the model suggests the novel possibility that synapses may possess private pools of external calcium that enforce some forms of short-term depression in a synapse-specific manner.

INTRODUCTION

Extracellular calcium plays a critical role in many neuronal processes, including the regulation and modulation of synaptic release events (Dittman and Regehr 1998; Mintz et al. 1995; Pumain 1998; Tsodyks and Markram 1997). Previous theoretical suggestions (Nicholson 1980) and computer simulation studies of external calcium dynamics, in which external calcium was free to move throughout the complicated interstices of the extracellular space (Eagleman 1998; Egelman and Montague 1998, 1999; Rusakov et al. 1999; Wiest et al. 2000), suggested that fluctuations in the level of extracellular calcium may constitute an information-bearing signal in the brain. The results of these modeling studies suggested in particular that while postsynaptic dendritic spiking activity was likely to decrement significantly local external calcium, electrically active presynaptic boutons were unable to significantly modulate the neighborhood calcium concentration.

The local geometry of brain tissue and the character of the extracellular matrix are unlikely to be as uniform as was assumed in these previous modeling studies. If small volumes of tissue were effectively isolated from the surrounding external calcium "bath," then presynaptic activity could permit normal neural activity to create fluctuations in the ionic composition within the enclosed spaces that are larger than ionic fluctuations under more open conditions. Given the known modulation of synaptic release by external calcium concentration, such modulation would contribute to short-term synaptic depression at any local presynaptic terminals.

Glial ensheathment provides one potential means of functionally isolating local volumes from the surrounding extracellular milieu. Excellent examples of well-defined glial ensheathment of synapses are found in the lateral geniculate nucleus (Wilson 1989), hippocampus (Shepherd and Harris 1998), cerebellum (Rossi and Hamann 1998), and retina (Stone et al. 1995). Calyx-type synapses offer another means to create isolated or quasi-isolated synaptic clefts by enveloping the postsynaptic dendrite locally. Recent experimental measurements of calcium currents at giant calyx-type synapses in chick ciliary ganglion (Stanley 2000) and rat brain stem (Borst and Sakmann 1999) provide strong evidence of calcium depletion in those synaptic clefts. Neither glia nor Calyceal synapses appear in serial electron-microscope reconstruction images to form tight seals around postsynaptic active zones; thus the experimental evidence that calcium depletion does occur (and mediates synaptic depression) in the clefts of Calyx-type synapses suggests that in vivo the seals may be tighter than they appear in electron-microscope reconstructions, or that other impediments to diffusion may cooperate with geometrical enclosures to create quasi-isolated compartments of tissue.

This paper uses a model of calcium diffusion in the extracellular space to show *1*) that structures that impede the diffusion-dependent replenishment of calcium in the synaptic cleft do increase the magnitude of calcium fluctuations at synapses, and *2*) that modulation of transmission probabilities via extracellular calcium depletion can account for published short-term synaptic depression data from cortical synapses.

METHODS

We model extracellular calcium consumption, diffusion, and replenishment using *1*) a finite-difference model and *2*) an analytic approximation. The finite-difference model allows direct simulation of the diffusion of extracellular calcium within a local volume of active units along with explicit representation of boundary conditions (such as the degree to which an extracellular volume is isolated from neighboring regions). However, this process is computationally expensive. The analytic approximation is efficient when average behavior, rather than detailed profiles of individual spikes, is desired, and when diffusion is not a major influence, i.e., when local volumes are effectively enclosed.

* R. D. King and M. C. Wiest contributed equally to this work.

Address for reprint requests: P. R. Montague, Center for Theoretical Neuroscience, Division of Neuroscience, Baylor College of Medicine, One Baylor Plaza, Houston, TX 77030 (E-mail: read@bcm.tmc.edu).

The costs of publication of this article were defrayed in part by the payment of page charges. The article must therefore be hereby marked "*advertisement*" in accordance with 18 U.S.C. Section 1734 solely to indicate this fact.

Finite difference model

The finite difference model of the extracellular space (called ***ECS***) (Egelman and Montague 1998) consists of intracellular and extracellular compartments, each of which holds a vector of state variables (calcium concentration, voltage, channel density, and channel activation parameters). Arranging and combining these compartments together at the appropriate scale permits us to incorporate three-dimensional neural elements such as boutons and dendrites. Diffusion in the finite difference model occurs with an effective diffusion constant of 200 $\mu m^2/s$ between contiguous extracellular compartments (Nicholson and Rice 1987; Wiest et al. 2000). Calcium consumption (through voltage-gated calcium channels) and replenishment (via 1st-order calcium pumps) occur between contiguous extracellular and intracellular compartments.

Three classes of Hodgkin-Huxley (H-H) type calcium channels were used: *1*) high-voltage activated, inactivating (N-like channel), *2*) high-voltage activated, noninactivating (L-like channel), and *3*) low-voltage activated, inactivating (T-like channel). A modified Goldman-Hodgkin-Katz model was used for the calcium current through each channel type j

$$I_j = \bar{P} \cdot A_j(V, t) \cdot \frac{4F^2}{RT} \cdot V \cdot \frac{[\mathrm{Ca}]_o - [\mathrm{Ca}]_i e^{2FV/RT}}{1 - e^{2FV/RT}}$$

$\bar{P}$ is the maximum calcium permeability, V is membrane voltage, t is time, $[\mathrm{Ca}]_o$ and $[\mathrm{Ca}]_i$ are the external and internal calcium concentrations, R is the universal gas constant, and F is Faraday's constant. The biophysical parameters of this model are based on experimentally measured values from several sources. The value of $\bar{P}$ was calibrated using experimental values (Helmchen et al. 1996) for the total calcium flux per unit area of membrane (Wiest et al. 2000). A_j is the H-H formulation for the jth type calcium channel, with $A_T(V, t) = m_T^2 h_T$, $A_N(V, t) = m_N^2 h_N$, and $A_L(V, t) = m_L^2$. In this formulation, $m_\infty = \alpha_m(\alpha_m + \beta_m)^{-1}$, $h_\infty = \alpha_h(\alpha_h + \beta_h)^{-1}$, and the αs and βs are all dependent on voltage and experimentally determined constants (Fisher et al. 1990; Jaffe et al. 1994; Verkhratsky and Kettenmann 1996). The voltage waveform used to drive the calcium channel models was recorded from a hippocampal CA1 pyramidal neuron soma (Poolos and Johnston 1999). The entire system of equations, including diffusion and calcium channel models, was integrated using a Runge-Kutta scheme. Further details and explanation of the ***ECS*** model can be found in Wiest et al. (2000).

Analytical model

The analytical model derived in this section is a simplified version of the finite-difference model. While it lacks the same degree of biophysical detail, it allows one to gain insight into the physical effects of glial enclosure. Let N and C be the number of intracellular and extracellular calcium ions, respectively. The evolution of internal and external calcium levels can be described by a pair of differential equations

$$\frac{\partial C}{\partial t} = F(C, N) + D\nabla^2 C \tag{1}$$

$$\frac{\partial N}{\partial t} = G(C, N) \tag{2}$$

where F and G are nonlinear functions of C and N. ∇^2 is the Laplacian operator that represents the spatial curvature of the external calcium concentration, and D is the effective diffusion coefficient for calcium. We consider the case of a single synapse or small group of synapses with access to a private pool of extracellular calcium; hence we set the $D\nabla^2 C$ term to 0 (no diffusion from neighboring regions). In such an enclosed volume, the total amount of calcium is conserved and must sum to a total value T. Thus $(\partial C/\partial t) = -(\partial N/\partial t)$. Linear approximation of *Eq. 1* with constant terms set to 0 yields

$$\frac{\partial C}{\partial t} = -\alpha C + \beta N \tag{3}$$

where $\alpha = (\partial F/\partial C)(0)$ and $\beta = (\partial F/\partial N)(0)$. Both of these parameters function as rate constants. The condition $C + n = T$ allows the substitution of $n = T - C$, which yields

$$\frac{\partial C}{\partial t} = -\alpha C + \beta(T - C) \tag{4}$$

Equation 4 can be separated and integrated to yield the following solution, where $C(t = 0) = C_0$

$$C(t) = \frac{\beta T}{\alpha + \beta} + \frac{C_0(\alpha + \beta) - \beta T}{\alpha + \beta} e^{-(\alpha+\beta)t} \tag{5}$$

In the case where $T \approx C_0$, *Eq. 5* simplifies to

$$C(t) = C_0\left[\frac{1}{1 + \alpha/\beta} + \frac{1}{1 + \beta/\alpha} e^{-(\alpha+\beta)t}\right] \tag{6}$$

Parameters for the analytical model

The constants α and β have a natural relationship to experimentally measured biological parameters. First-order calcium pumps mediate the extrusion of calcium from the inside of the synapse into the extracellular space at a rate proportional to the amount of internal calcium. The constant β is therefore inverse of the time constant (τ) of these calcium pumps. Experimentally, the parameter τ is on the order of 100–500 ms (Philipson and Nicoll 1993; Schatzmann 1989). We estimate α by taking the influx of calcium as proportional to the product of the external calcium level and the rate of action potential invasion. Thus $\alpha = \kappa r$, where κ is a dimensionless scaling parameter that characterizes the amount of calcium intake per spike. The value of κ is less constrained by experimental data. In *dendrites*, the range of κ may be estimated by dividing the experimentally measured values of the number of calcium atoms consumed per spike per square micrometer of membrane (Helmchen et al. 1996) by the total number of calcium ions in the cleft. This leads to a rough range for κ from 0.18 to 1.0. Using a value from this range in our model, we can match the steady-state depression data but not the time course as reported by Abbott et al. (1997) (not shown). To account for the spike-by-spike data, we must assume that κ is around 0.1 (see Fig. 6). This choice implies that synaptic terminals consume less calcium per square micrometer of membrane than do dendrites, consistent with other observations (Rusakov et al. 1999).

The firing rate r represents a fixed increase from an initial rate R_o to a new rate R. In the case where the initial rate R_o is nearly zero, such as in cortical slices, r equals R. Substituting these biological constants into *Eq. 6* yields

$$C(r, t) = C_0\left[\frac{1}{1 + \tau\kappa r} - \frac{1}{1 + (\tau\kappa r)^{-1}} e^{-(\tau+\kappa r)t}\right] \tag{7}$$

In words, *Eq. 7* characterizes the influence of a step change in the firing rate on the time course of external calcium fluctuations. As a final step, *Eq. 7* can be divided by the volume of the extracellular space (V_{cleft}) to yield the results in terms of concentration.

RESULTS

Enclosure amplifies and prolongs the calcium decrement

We used a finite-difference model to calculate the expected calcium decrement around two asynchronously active boutons

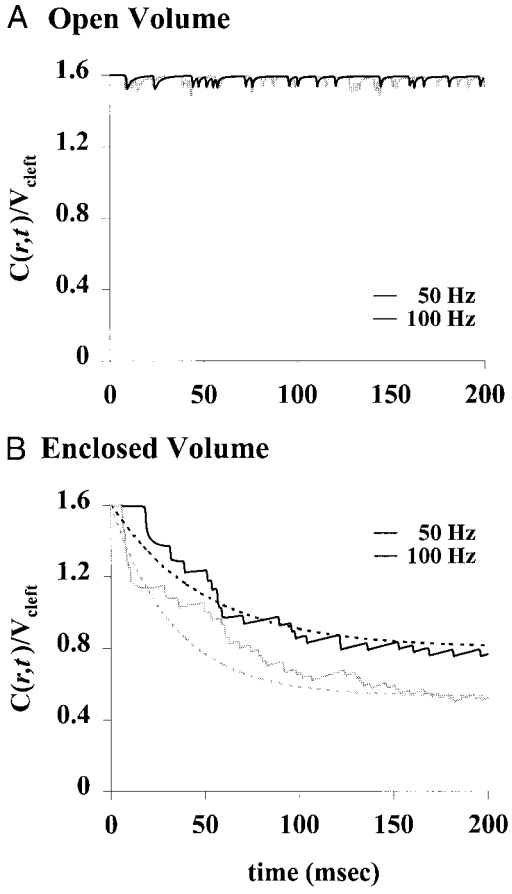

FIG. 1. Open vs. closed geometric conditions. Extracellular calcium concentration through time computed by the finite-difference model for a range of firing rates. There are 2 active boutons in the simulation, each firing with an independent Poisson spike train (black line, 50 Hz; gray line, 100 Hz). If multiple boutons cohabit a given enclosure, the possibility arises for conditional interactions among terminals, in addtion to the individual short-term depression effect, which is the focus of this study. *A*: open volume; the 2 boutons are contained within a $7 \times 7 \times 7$ volume (each modeled tissue unit is a cube 0.826 μm on a side) with no enclosures around the pair. *B*: enclosed volume; same parameters as in *A*, except that the clefts around 2 boutons are closed off from the outer $7 \times 7 \times 7$ volume. Without the diffusion of calcium from the neighboring volume, the calcium is depleted from the extracellular space within the enclosure. Dotted lines: analytic approximation of the external calcium concentration inside an enclosed volume, using *Eq. 7*. The analytical model approximates the finite-difference model by assuming *1*) continuous calcium consumption instead of discrete consumption events, and *2*) each spike consumes independently of every other spike (i.e., there is no refractory period after a spike).

over a range of Poisson firing rates under the following boundary conditions: *1*) there are no physical barriers to impede diffusion from replenishing the calcium consumed during synaptic activation, or *2*) the bouton pair is fully ensheathed, with the only calcium replenishment into the extracellular space coming from first-order calcium pumps. The results are shown in Fig. 1. An enclosure around two boutons amplifies the calcium decrement for any given firing rate, and prolongs the rate of recovery following stimulation (the latter not shown). An analytic solution, which is derived for the enclosed case, is shown as the dashed curves in Fig. 1. The analytic calcium profiles resemble the finite difference model under enclosed conditions (Fig. 1*B*), suggesting that the analytical approximations are appropriate over a physiological range of firing rates.

Degrees of enclosure: diffusion in the finite difference model

Given that restricting the diffusion of calcium around boutons amplifies the calcium decrement, how does the degree of enclosure affect the size of the extracellular calcium signal? We can set the degree to which diffusion is limited using partially open geometrical conditions in the finite difference model (Fig. 2). We model increased isolation by scaling the calcium flux between enclosed and open cleft units by γ, which indicates the percentage of diffusion paths that are available. For a completely isolated space, $\gamma = 0$, while $\gamma = 1$ for the maximally open condition. Within the enclosure, $D = 200$ $\mu m^2/s$, which is the effective diffusion constant of calcium in the extracellular space (Nicholson and Rice 1987; Wiest et al. 2000), and $\gamma = 1$. As shown in Fig. 2, when $\gamma = 0.01$, the calcium transient is amplified but returns quickly to baseline levels. When $\gamma < 0.0005$, there is both an amplification of the calcium signal for each spike, as well as a significant drop in the steady-state calcium level around the synapse. As expected, when enclosure has a greater degree (i.e., γ is smaller), the steady-state level of extracellular calcium will drop lower for any given firing rate.

Encoding the rate of activity into the level of extracellular calcium

The fact that every spike causes fluctuations in the extracellular calcium level suggests a novel information-bearing role for calcium: measuring the calcium level in a local region gives a measure of how electrically active that region is (Wiest et al. 2000). The relationship between the steady-state calcium level (C_{ss}) and the rate, as taken from Fig. 1, *A* and *B*, is shown in Fig. 3. We can see that there is a region in the plot in which the

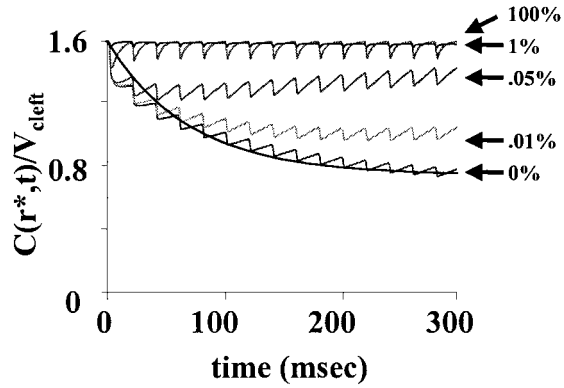

FIG. 2. Degrees of enclosure. Time course of external calcium levels in the model outside a single bouton firing at rate $r^* = 50$ Hz (where * indicates that the parameter is fixed; jagged lines). A variable percentage of the possible paths by which calcium diffusion could occur are available. In the open condition (100%, $\gamma = 1$), diffusion quickly replenishes the external calcium taken into the terminal, and thus there is no sustained decrement in external calcium at this firing rate. In the closed case (0%, $\gamma = 0$), there is no diffusion from surrounding regions to replenish the calcium consumed during the action potential, and recovery takes place exclusively via 1st-order extrusion pumps. The range of reported time constants for the calcium extrusion pumps matches the time courses for recovery from short-term depression. Three partially open conditions (1–0.01%, $\gamma = 0.01$–0.0001) are also shown. The smooth black line is *Eq. 7*, as computed from the analytical model ($C' = 1.6$ mM, $\kappa = 0.15$, $\tau = 300$, $r^* = 50$ Hz). The effective diffusion constant must be reduced to well below 0.01% of the open condition to obtain values that are consistent with the analytical model. However, significant calcium decrements are seen with diffusion reduced to 1% of the effective value.

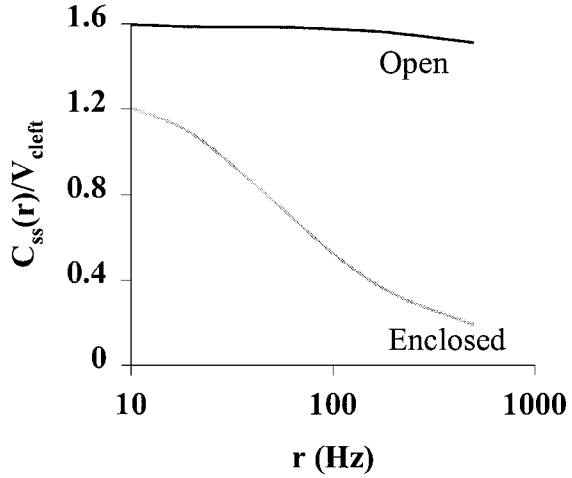

FIG. 3. Logarithmic relation between firing rate and extracellular calcium. The vertical axis represents the steady-state level of external calcium measured between a pair of boutons activating over a range of firing rates. The steady-state external calcium level was estimated as the average value between 190 and 200 ms. In the open condition (black line), there is very little change in the external calcium level because calcium is quickly replenished via diffusion from neighboring clefts. In contrast, enclosed boutons drop the local external calcium to a much lower level than in the open condition. When graphed on a semi-log plot, there is a nearly linear region in the relation between external calcium and the firing rate. This relationship is characterized in *Eqs. 8* and *9*. Enclosing the boutons greatly increases the slope of the log relation (from $\eta = 0.08$ to $\eta = 0.26$).

level of extracellular calcium is a linear function of the change in firing rate plotted on a logarithmic scale.

$$C_{ss}(r) = -\eta \log (r/R_c) + C_{ss}(R_c) \quad (8)$$

or

$$c_{ss}(r) = -\eta \log (r/R_c) + \epsilon \quad (9)$$

where $c_{ss}(r) = C_{ss}(R) - C_0$, and $\epsilon = C_{ss}(R_c) - C_0$. R_c represents the lowest frequency for which the linear relation holds (~10 Hz; see Fig. 3); r must be positive (i.e., $R > R_o$) and greater than R_c for the log relationship to be valid. The time it takes to reach this regime depends on the rate of firing (i.e., with faster firing rates, it takes less time to reach the linear regime). We estimate that it takes from 5 to 10 spikes before the calcium depletion is in the linear regime, based on the time needed to reach steady state in Fig. 1. Note that the log relationship holds in both the open and enclosed conditions, with the enclosure changing the slope from $\eta \approx 0.08$ to $\eta \approx 0.26$. However, in the open case, the change in the external calcium concentration is probably too small to be detected, based on previous estimates of the minimum detectable fluctuation (Egelman and Montague 1999; Wiest et al. 2000).

One consequence of the log relation is that doubling any rate (as long as the rate is still in the linear regime) in a volume will always create the same size fluctuation in calcium level (i.e., changing from 10 to 20 Hz will create the same size signal as changing from 40 to 80 Hz).

External calcium and synaptic transmission probabilities

The probability of a synapse transmission given an action potential (P_T) has been measured using optical techniques (Mintz et al. 1995; Qian et al. 1997); see Fig. 4. Our analysis of this data shows synaptic transmission probability to be proportional to the square of the extracellular calcium level

$$P_T = \nu([\mathrm{Ca}]_e)^2 \quad (10)$$

where $\nu = 0.24\ \mathrm{mM}^{-2}$. Thus fluctuations in the level of calcium would amount to changes in the square root of synaptic transmission probability. Substituting in the analytical approximation for the external calcium level as a function of an increase in firing rate (r) in an enclosed volume (*Eq. 7*, see

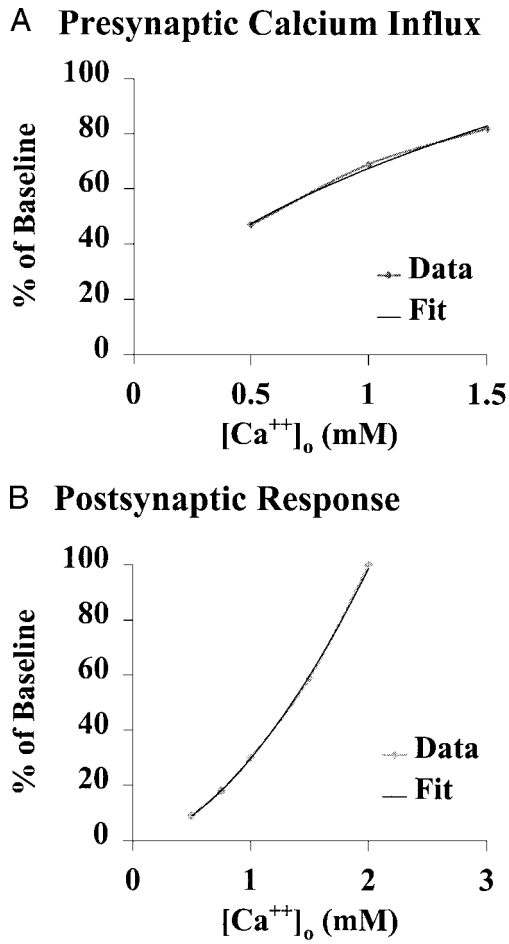

FIG. 4. Relationship between external calcium and postsynaptic response. *A*: presynaptic calcium influx measured using fluorescent dyes (adapted from Qian et al. 1997). To determine the relationship between presynaptic calcium influx and the level of extracellular calcium, Qian et al. filled hippocampal presynaptic terminals with either Fura or Furaptura. The terminals were activated under a range of bath extracellular calcium conditions. The normalized magnitude of the presynaptic fluorescent signal (**y**) is sublinear with respect to the extracellular calcium concentration (**x**) (Furaptra, $\mathbf{y} = 68\mathbf{x}^{0.51}$, $R^2 = 0.9957$). When this square-root relationship is combined with the relationship between presynaptic calcium influx and synaptic vesicle release, which is known to be 4th order in calcium (Heidelberger et al. 1994), then the predicted relationship between the external calcium level and synaptic vesicle release is ~2nd order. *B*: postsynaptic response as a function of external calcium (adapted from Qian et al. 1997). The postsynaptic response (**y**), as assayed by field excitatory postsynaptic potential, accrues a roughly quadratic dependence on external calcium (**x**) within the physical range of calcium concentrations ($\mathbf{y} = 0.24\mathbf{x}^{2.01}$, $R^2 = 0.9996$). Mintz et al. (1995) found similar results ($\mathbf{y} = 0.30\mathbf{x}^{1.72}$, $R^2 = 0.9998$).

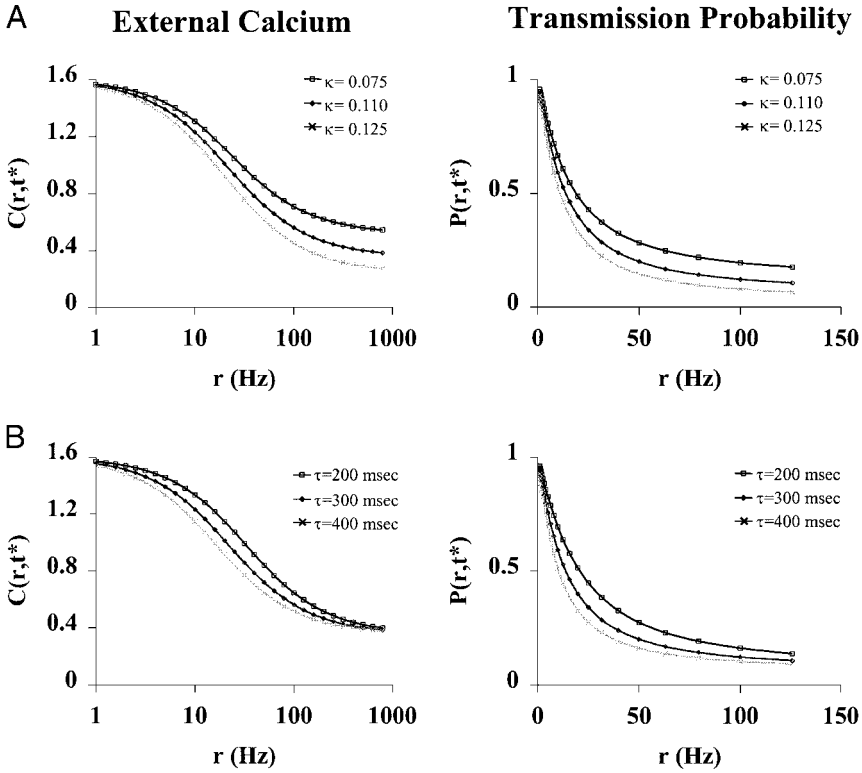

FIG. 5. External calcium theory for changes in probability of neurotransmission. *A*: sensitivity to calcium consumption rate. *Left*: theoretical dependence of external calcium on changes in firing rate as determined by *Eq. 7* for an enclosed tissue volume. The 3 lines demonstrate the sensitivity of *Eq. 7* to the rate of calcium consumption κ ($0.075 < \kappa < 0.125$). The calcium extrusion pump time constant $\tau = 300$ ms, and the resting external calcium level $C' = 1.6$ mM. The asterisk denotes that the variable is held constant. t^* represents the time to reach 15 spikes at the respective rate; this was done to correspond with experimental results (Abbott et al. 1997; Tsodyks and Markram 1997). *Right*: theoretical dependence of normalized transmission probability on firing rate. This relationship accrues due to the predicted changes in external calcium shown in the *left panel*, and is characterized by *Eq. 11*. The sensitivity to varying κ is again shown in this panel. *B*: sensitivity to calcium extrusion rate. The *left* and *right panels* are the same as in *A*, except that the sensitivity to τ (200 ms $< \tau <$ 400 ms) is demonstrated for a fixed $\kappa = 0.11$. Variability in τ and κ may account for some of the heterogeneity seen in the degree of depression among cortical synapses.

METHODS, but note that $\tilde{C}_0$ represents concentration rather than a number of ions), we obtain

$$P_T = \nu\left\{\tilde{C}_0\left[\frac{1}{1+\tau\kappa r} - \frac{1}{1+(\tau\kappa r)^{-1}}\,e^{-(\tau+\kappa r)t}\right]\right\}^2 \qquad (11)$$

Equation 11 is the dependence of synaptic transmission probability on firing rate, time, and initial calcium concentration for values of τ and κ. Using *Eq. 7*, we plot the external calcium level as a function of the change in action potential rate r over a range of values for τ and κ (Fig. 5, *left column*). The resulting transmission probabilities of synapses feeling the calcium level, as quantified by *Eq. 11*, are also shown in Fig. 5 (*right column*). The functions are evaluated at a time t^*, which corresponds to the time required to reach 15 spikes at the respective firing rates.

Altered release probability as a model for short-term synaptic depression

The temporal profile of synaptic transmission probability characterized in *Eq. 11* bears striking resemblance to a particular form of short-term synaptic depression exhibited by synapses in the cerebral cortex (Abbott et al. 1997; Tsodyks and Markram 1997; Varela et al. 1997). The basic observation about this form of synaptic plasticity is that once a synaptic terminal has fired, its subsequent likelihood of transmitting is decreased. This observation has been made in different contexts and with different recording techniques (Abbott et al. 1997; Tsodyks and Markram 1997; Varela et al. 1997).

We used the relationships shown in Fig. 5 to compare the predictions of the model to the experimental results of Tsodyks and Markram (Fig. 6*A*) and Abbott et al. (Fig. 6, *B–D*). The proposed mechanism matches the data at low and high frequencies. With one further assumption about the scaling of the κ consumption parameter (Fig. 6*A*, legend), the model also provides a quantitative match to the dependence of synaptic depression on external calcium levels as reported by Tsodyks and Markram (Fig. 6*A*). The time course of recovery from depression, as described by *Eq. 7*, depends on the time constant of the calcium pumps (Schatzmann 1989) (τ), which places it well within the range of recovery times reported in other studies (Abbott et al. 1997; Dittman and Regehr 1998; Tsodyks and Markram 1997). It should be noted that and τ and κ are parameters whose range was estimated from independent experiments unrelated to assessments of synaptic depression (see METHODS).

The depletion of calcium from the extracellular space also places a constraint on density of synaptic transmissions per unit time per unit tissue volume. The average number of transmissions that occurs per second is equal to the number of spikes that occur per second (rate) times the probability of transmission per spike (P_T). As shown in Fig. 7, the probability of transmission (P_T) is approximately equal to the inverse of the firing rate times a constant (χ) at rates of $r > \sim 40$ Hz. Therefore

$$\frac{\text{number of transmissions}}{\text{second}} = rP_T = r\nu[\text{Ca}]^2 = r\chi(1/r) = \chi \qquad (12)$$

In this view, calcium acts as a normalizing fluid that sets the total number of transmissions in an enclosed volume to a constant level. Such an arrangement would enable the tissue to register changes in slow firing inputs as well as rapidly firing inputs (Abbott et al. 1997).

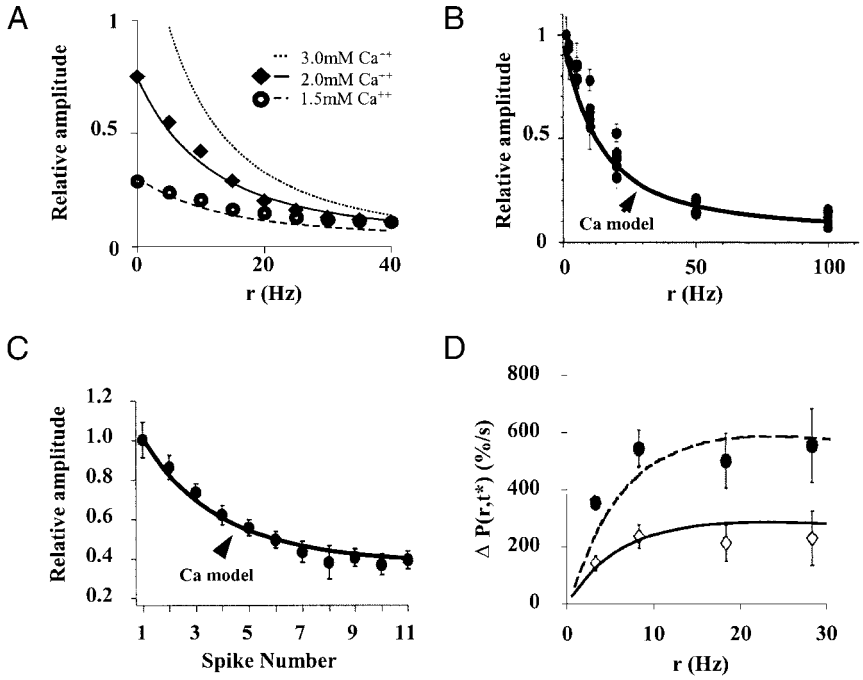

FIG. 6. External calcium model compared with experimental results from 2 sources. *A*: theoretical changes in transmission probability resulting from external calcium decrements matches experimental data from cortical synapses. The diamonds and circles are data points adapted from Tsodyks and Markram (1997). The solid lines are *Eq. 11*. The model as described captures both the steady-state response and the time course of the postsynaptic response (see also *B* and *C*). With one other assumption we can capture the influence of initial external calcium concentration on the steady-state amplitude of the postsynaptic current, and the fact that the relative depression is greater when the calcium concentration is higher, which is consistent with Varela et al. (1997). In particular, we scale the value of κ by the ratio of the external calcium concentrations: *top trace*: $C' = 3$ mM, $\kappa = 0.21$, $\tau = 300$ ms, $\eta = 2$; *middle trace*: $C' = 2$ mM, $\kappa = 0.14$, $\tau = 300$ ms, $\eta = 2$; *bottom trace*: $C' = 1.5$ mM, $\kappa = 0.105$, $\tau = 300$ ms, $\eta = 2$. *B*: the experimental data in *B–D* are adapted from Abbott et al. (1997). The circles in *B* are measurements of the relative amplitude of extracellular field potentials after activation across a range of firing rates with 15 spikes. The solid line (same solid line as in Fig. 5, *A* and *B*, *right*) shows the prediction of the analytical model (*Eq. 11;* $C' = 1.6$ mM, $\kappa = 0.11$, $\tau = 300$ ms, $\eta = 2$). *C*: the time course of the depression predicted by *Eq. 5* matches experimental data when plotted spike by spike (circles, synapses activated at 20 Hz). The parameter settings are the same as in *B*, except that we permit t to vary and fix r^* at 20 Hz. *D*: the change in release probability (ΔP) due to instantaneous rate changes from r to $r + \Delta r$ for 2 different values of the ratio $\Delta r/r$. The changes are of constant magnitude for constant ratios of $\Delta r/r$. For example, the response due to a rate change from 10 to 20 Hz is the same magnitude as the response from 20 to 40 Hz. Consequently, changing the rate by a constant amount will produce successively smaller increases in response. Dotted line: changes in rate by a factor $\Delta r/r = 1$; solid line: changes in rate by a factor $\Delta r/r = 0.5$. Parameter settings are the same as in *B*.

DISCUSSION

Our simulations show that barriers to calcium diffusion in the extracellular space of brain tissue could modulate changes in external calcium during neural activity, suggesting that isolated calcium pools around synapses could be used computationally. We also found that spike activity in an enclosed tissue volume is integrated and encoded logarithmically in the external calcium level. This measure of average local activity is thus available for further processing by neurons or glial cells (Verkhratsky and Kettenmann 1996). For example, the logarithmic dependence of the external calcium level on neural firing rate could provide a natural medium for computing products. Consistent with this possibility, Gabbiani et al. (1999) argued that multiplication performed in the cricket "looming" detector system uses a logarithmic representation.

If the information encoded in external calcium fluctuations is actually used in brain computations, then there must exist physiological "readers" of the external calcium concentration. Consistent with this general hypothesis, many important brain processes are sensitive to external calcium levels. One focus of this paper has been neurotransmission, which depends strongly on extracellular calcium (Katz and Miledi 1970; Mintz et al. 1995; Qian et al. 1997). In addition, ionotropic receptors (Xiong et al. 1997) and metabotropic receptors (Brown et al. 1995; Kubo et al. 1998) can be activated by changes in extracellular calcium. Gap-junctional hemichannels were found to regulate cell volume in response to changes in extracellular calcium (Quist et al. 2000). Other external calcium-dependent processes include cell adhesion (Rose 1998; Tang et al. 1998; Uemura 1998) and synaptic plasticity (Bear and Malenka 1994; Denk et al. 1996), both of which could involve glial calcium signaling (Verkhratsky and Kettenmann 1996).

Synaptic depression: comparing extracellular calcium to other mechanisms

Our results demonstrate the biophysical plausibility of external calcium depletion as a mechanism of short-term synaptic depression; however, they do not exclude mechanisms internal to the synapse, such as the depletion of vesicle pools, which are believed to be involved in synaptic depression (Castro-Alamancos and Connors 1997; Dobrunz and Stevens 1997;

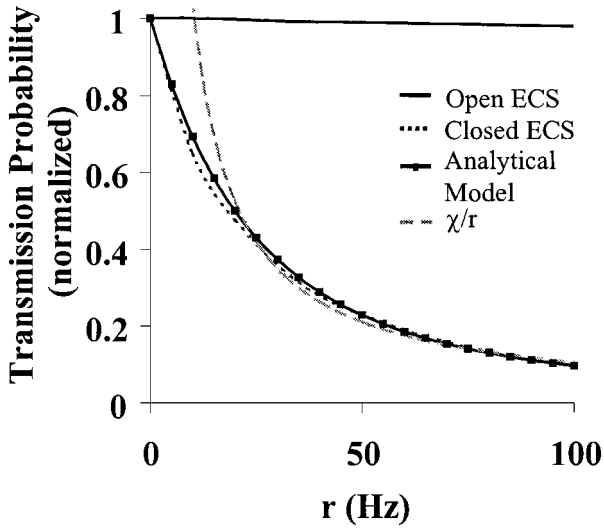

FIG. 7. External calcium depletion relates firing rate to experimentally measured transmission probability. Normalized transmission probabilities for synaptic terminals in the open (black solid) and closed (black dotted) geometric conditions, computed from the calcium profiles generated from the ***ECS*** model and *Eq. 10* (averaging the calcium concentration between 250 and 300 ms of stimulation time). Black line with squares: analytical model under the same conditions (*Eq. 11;* $C' = 1.6$ mM, $\kappa = 0.15$, $\tau = 300$, $t^* = 300$ ms). Gray dashed line: $1/r$ times the proportionality constant $\chi = 10$. Below ~40 Hz, the $1/r$ model deviates from the analytical model.

Dobrunz et al. 1997; Markram et al. 1998). In fact, synaptic depression can be observed in dissociated tissue culture, where local calcium depletion is unlikely to occur. However, models that do not take into account external calcium changes cannot explain the scaling of the rate of synaptic depression with the external calcium level (Dittman and Regehr 1998). This omission is relevant in light of ion-sensitive microelectrode measurements that consistently show significant changes in external calcium in response to neural stimulation in vitro (Benninger et al. 1980; Heinemann et al. 1990; Pumain and Heinemann 1985; Stanton and Heinemann 1986) and in vivo (Nicholson et al. 1978).

An empirical distinction exists between our proposed external calcium mechanism and other mechanisms of synaptic depression, such as vesicle depletion, which may help to determine to what extent a given synapse is influenced by external calcium depletion. Vesicle depletion would occur only at synapses that actually transmit during a given action potential (release-dependent depression), whereas external calcium depletion alters the transmission probability even if no previous transmissions have occurred (release-independent depression). Ideally, to distinguish these cases experimentally, one would record the calcium and transmission activities of individual synapses. Nevertheless, electrophysiological recordings at multi-synaptic connections have already demonstrated the existence of release-independent synaptic depression, incompatible with a simple vesicle depletion model (Brody and Yue 2000; Waldeck et al. 2000). In the first study (Brody and Yue 2000), hippocampal cultured autapses exhibited depression inconsistent with a vesicle depletion hypothesis, but also unlikely to be due to external calcium depletion. The authors favored an action-potential failure mechanism, operating at axonal branch points. On the other hand, the observation by Waldeck et al. of paired-pulse depression at a goldfish brain stem connection was inconsistent with vesicle depletion but appears consistent with a contribution from external calcium depletion. Multiple mechanisms of short-term synaptic plasticity are likely to be at work in varying degrees at each synapse in a particular brain.

Recent experiments that measured the external calcium currents at the chick ciliary ganglion suggested significant external calcium depletion of the synaptic cleft (Stanley 2000). Similarly, Borst and Sakmann (1999) measured pre- and postsynaptic calcium currents at a calyx-type synapse in rat brain stem, together with postsynaptic potentials, demonstrating synaptic depression in parallel with declining presynaptic calcium currents (or barium currents, to minimize calcium messenger effects). The current required to achieve synaptic depression suggested that the calyx synaptic clefts are not perfectly isolated from calcium in the surrounding tissue, and there may be unknown reserves of calcium in the extracellular space. However, we expect synchronous firing (Egelman and Montague 1998, 1999; Wiest et al. 2000) or bursts of action potentials, which we did not model here, to deplete external calcium faster than the independent action potentials we modeled. This expectation is confirmed experimentally for massive synchronous activation during epileptic seizures (Pumain et al. 1983). The recruitment of *N*-methyl-D-aspartate (NMDA) receptor activity would likewise contribute to greater external calcium depletion than we found, since the present model included only voltage-gated calcium channels.

Computational role for glial-defined spaces

Our results raise the question of the nature of the hypothesized barriers to diffusion in the extracellular space. Glial investments around synapses could create a compartment in which local external calcium fluctuates rapidly due to spike activity, yet equilibrates on a slower time scale with the surrounding regions of the extracellular space. Other factors, such as extracellular matrix molecules, could contribute to slowing diffusion or to holding glia in place. For a fixed rate of calcium extrusion, changes in the private external volume available to each synapse could provide sensitive control over the effective local levels of external calcium. Consequently, local structural modulation could act to modulate those parts of short-term depression controlled by changes in external calcium levels (Fields et al. 1987; Hosokawa et al. 1997). Complex calcium signaling pathways between glial cells and neurons support such an interpretation (Verkhratsky and Kettenmann 1996). While our model cannot predict the relative importance of various possible barriers to diffusion around particular synapses, the current results suggest one novel computational role for glia in segregating (different compartments) and integrating (within a compartment) information coded in the external calcium level.

We gratefully acknowledge the helpful conversations and technical advice of S. McClure as well as Drs. David Eagleman, Michael Mauk, J. David Sweatt, and Jim Patrick.

This work was supported by the Center for Theoretical Neuroscience at the Baylor College of Medicine, by National Institutes of Health Grants

MH-52797 and DA-11723 to P. R. Montague, by the United Negro College Fund/Merck Foundation and NIH Grant MH-19547 to R. D. King, and by the Biomedical Computation and Visualization Laboratory at the Baylor College of Medicine (NSF-BIR-9412521). M. C. Wiest is a Kane Foundation Fellow and is supported by NIH Grant 1T15LM-07093 through the Keck Center for Computational Biology.

REFERENCES

ABBOTT LF, VARELA JA, SEN K, AND NELSON SB. Synaptic depression and cortical gain control. *Science* 275: 220–224, 1997.

BEAR MF AND MALENKA RC. Synaptic plasticity: LTP and LTD. *Curr Opin Neurobiol* 4: 389–399, 1994.

BENNINGER C, KADIS J, AND PRINCE D. Extracellular calcium and potassium changes in hippocampal slices. *Brain Res* 187: 165–182, 1980.

BORST JGG AND SAKMANN B. Depletion of calcium in the synaptic cleft of a calyx-type synapse in the rat brainstem. *J Physiol (Lond)* 521: 123–133, 1999.

BRODY D AND YUE D. Release-independent short-term synaptic depression in cultured hippocampal neurons. *J Neurosci* 20: 2480–2494, 2000.

BROWN EM, VASSILEV PM, AND HERBERT SC. Calcium ions as extracellular messengers. *Cell* 83: 679–682, 1995.

CASTRO-ALAMANCOS MA AND CONNORS BW. Distinct forms of short-term plasticity at excitatory synapses of hippocampus and neocortex. *Proc Natl Acad Sci USA* 95: 4161–4166, 1997.

DENK W, YUSTE R, SVOBODA K, AND TANK DW. Imaging calcium dynamics in dendritic spines. *Curr Opin Neurobiol* 6: 372–378, 1996.

DITTMAN J AND REGEHR W. Calcium dependence and recovery kinetics of presynaptic depression at the climbing fiber to purkinje cell synapse. *J Neurosci* 18: 6147–6162, 1998.

DOBRUNZ LE AND STEVENS CF. Heterogeneity of release probability, facilitation, and depletion at central synapses. *Neuron* 18: 995–1008, 1997.

DOBRUNZ LF, HUAN EP, AND STEVENS CF. Very short-term plasticity in hippocampal synapses. *Proc Natl Acad Sci USA* 95: 14843–14847, 1997.

EAGLEMAN DM. *Computational Properties of Extracellular Calcium Dynamics* (PhD dissertation). Houston, TX: Baylor College of Medicine, 1998.

EGELMAN DM AND MONTAGUE PR. Computational properties of peri-dendritic calcium fluctuations. *J Neurosci* 18: 8580–8589, 1998.

EGELMAN DM AND MONTAGUE PR. Calcium dynamics in the extracellular space of mammalian neural tissue. *Biophys J* 76: 1856–1867, 1999.

FIELDS RD, ELLISMAN MH, AND WAXMAN SG. Changes in synaptic morphology associated with presynaptic and postsynaptic activity: an in vitro study of the electrosensory organ of the thornback ray. *Synapse* 1: 335–346, 1987.

FISHER RE, GRAY R, AND JOHNSTON D. Properties and distribution of single voltage-gated calcium channels in adult hippocampal neurons. *J Neurophysiol* 64: 91–104, 1990.

GABBIANI F, KRAPP H, AND LAURENT G. Computation of object approach by a wide-field, motion-sensitive neuron. *J Neurosci* 19: 1122–1141, 1999.

HEIDELBERGER R, HEINEMANN C, NEHER E, AND MATTHEWS G. Calcium dependence of the rate of exocytosis in a synatic terminal. *Nature* 371: 513–515, 1994.

HEINEMANN U, STABEL J, AND RAUSCHE G. Activity-dependent ionic changes and neuronal plasticity in rat hippocampus. *Prog Brain Res* 83: 197–214, 1990.

HELMCHEN F, IMOTO K, AND SAKMANN B. Ca^{2+} buffering and action-potential–evoked Ca^{2+} signalling in dendrites of pyramidal neurons. *Biophys J* 70: 1069–1081, 1996.

HOSOKAWA T, RUSAKOV DA, BLISS TV, AND FINE A. Repeated confocal imaging of individual dendritic spines in the living hippocampal slice: evidence for changes in length and orientation associated with chemically induced LTP. *J Neurosci* 15: 5560–5573, 1997.

JAFFE DB, ROSS WN, LISMAN JE, LASSER-ROSS N, MIYAKAWA H, AND JOHNSTON D. A model for dendritic Ca^{2+} accumulation in hippocampal pyramidal neurons based on fluorescence imaging measurements. *J Neurophysiol* 71: 1065–1077, 1994.

KATZ B AND MILEDI R. Further study of the role of calcium in synaptic transmission. *J Physiol (Lond)* 207: 789–801, 1970.

KUBO Y, MIYASHITA T, AND MURATA Y. Structural basis for a Ca^{2+}-sensing function of the metabotropic glutamate receptors. *Science* 279: 1722–1725, 1998.

MARKRAM H, WANG Y, AND TSODYKS M. Differential signaling via the same axon of neocortical pyramidal neurons. *Proc Natl Acad Sci USA* 95: 5323–5328, 1998.

MINTZ I, SABATINI B, AND REGEHR W. Calcium control of transmitter release at a central synapse. *Neuron* 15: 675–688, 1995.

NICHOLSON C. Modulation of extracellular calcium and its functional implications. *Federation Proc* 39: 1519–1523, 1980.

NICHOLSON C AND RICE ME. Calcium diffusion in the brain cell microenvironment. *Can J Physiol Pharmacol* 65: 1086–1091, 1987.

NICHOLSON C, TEN BRUGGENCATE G, STOCKLE H, AND STEINBERG R. Calcium and potassium changes in extracellular microenvironments of cat cerebellar cortex. *J Neurophysiol* 41: 1026–1039, 1978.

PHILIPSON K AND NICOLL D. Molecular and kinetic aspects of sodium-calcium exchange. *Int Rev Cytol* 137C: 199–227, 1993.

POOLOS NP AND JOHNSTON D. Calcium-activated potassium conductances contribute to action potential repolarization at the soma but not the dendrites of hippocampal CA1 pyramidal neurons. *J Neurosci* 19: 5205–5212, 1999.

PUMAIN R. Calcium ions. In: *The Neuronal Microenvironment*, edited by Boulton AA, Baker GB, and Walz W. Clifton, NJ: Humana, 1998, vol. 9, p. 589–641.

PUMAIN R AND HEINEMANN U. Stimulus- and amino acid-induced calcium and potassium changes in rat neocortex. *J Neurophysiol* 53: 1–16, 1985.

PUMAIN R, KURCEWICZ I, AND LOUVEL J. Fast extracellular calcium transients: involvement in epileptic processes. *Science* 222: 177–179, 1983.

QIAN J, COLMERS WF, AND SAGGAU P. Inhibition of synaptic transmission by Neuropeptide Y in rat hippocampal area CA1: modulation of presynaptic calcium entry. *J Neurosci* 17: 8169–8177, 1997.

QUIST AP, RHEE SK, LIN H, AND LAL R. Physiological role of gap-junctional hemichannels. Extracellular calcium-dependent isosmotic volume regulation. *J Cell Biol* 148: 1063–1074, 2000.

ROSE S. Cell-adhesion molecules, glucocorticoids and long-term memory formation. *Trends Neurosci* 18: 502–506, 1998.

ROSSI DJ AND HAMANN M. Spillover-mediated transmission at inhibitory synapses promoted by high affinity alpha6 subunit GABAa receptors and glomerular geometry. *Neuron* 20: 783–795, 1998.

RUSAKOV DA, KULLMANN DM, AND STEWART MG. Hippocampal synapses: do they talk to their neighbors? *Trends Neurosci* 22: 382–388, 1999.

SCHATZMANN H. The calcium pump of the surface membrane and of the sarcoplasmic reticulum. *Annu Rev Physiol* 51: 473–485, 1989.

SHEPHERD GM AND HARRIS KM. Three-dimensional structure and composition of CA3 → Ca1 axons in rat hippocampal slices: implications for presynaptic connectivity and compartmentalization. *J Neurosci* 18: 8300–8310, 1998.

STANLEY EF. Presynaptic calcium channels and the depletion of synaptic cleft calcium ions. *J Neurophysiol* 83: 477–482, 2000.

STANTON P AND HEINEMANN U. Norepinephrine enhances stimulus-evoked calcium and potassium concentration changes in dendate granule cell layer. *Neurosci Lett* 67: 233–238, 1986.

STONE J, MARKOV F, AND HOLLANDER H. The glial ensheathment of soma and axon hillock of retinal ganglion cells. *Vis Neurosci* 12: 273–279, 1995.

TANG L, HUNG CP, AND SCHUMAN EM. A role for the cadherin family of cell adhesion molecules in hippocampal long-term potentiation. *Neuron* 20: 1165–1175, 1998.

TSODYKS M AND MARKRAM H. The neural code between neocortical pyramidal neurons depends on neurotransmitter release probability. *Proc Natl Acad Sci USA* 94: 719–723, 1997.

UEMURA T. The cadherin superfamily at the synapse: more members, more missions. *Cell* 93: 1095–1098, 1998.

VARELA JA, SEN K, GIBSON J, FOST J, ABBOT LF, AND NELSON SB. A quantitative description of short-term plasticity at excitatory synapses in layer 2/3 of rat primary cortex. *J Neurosci* 17: 7926–7940, 1997.

VERKHRATSKY A AND KETTENMANN H. Calcium signalling in glial cells. *Trends Neurosci* 19: 346–352, 1996.

WALDECK R, PEREDA A, AND FABER D. Properties and plasticity of paired-pulse depression at a central synapse. *J Neurosci* 20: 5312–5320, 2000.

WIEST MC, EGELMAN DM, KING RD, AND MONTAGUE PR. Dendritic spikes and their influence on extracellular calcium signaling. *J Neurophysiol* 83: 1329–1337, 2000.

WILSON JR. Synaptic organization of individual neurons in the macaque lateral geniculate nucleus. *J Neurosci* 9: 2931–2953, 1989.

XIONG Z-G, LU W-Y, AND MACDONALD JF. Extracellular calcium sensed by a novel cation channel in hippocampal neurons. *Proc Natl Acad Sci USA* 94: 7012–7017, 1997.